Adaptive Power Allocation Scheme for Mobile NOMA Visible Light Communication System

Zanyang Dong * , **Tao Shang ***, **Qian Li** and **Tang Tang**

State Key Laboratory of Integrated Service Networks, School of Telecommunications Engineering,
Xidian University, Xi'an 710071, China; liqian_xd@foxmail.com (Q.L.); tangt_xd@foxmail.com (T.T.)
* Correspondence: zanydong@foxmail.com (Z.D.); tshang@xidian.edu.cn (T.S.);
  Tel.: +86-187-1084-6102 (Z.D.); +86-134-6893-5375 (T.S.)

check for
updates

Abstract: Recently, due to its higher spectral efficiency and enhanced user experience, non-orthogonal multiple access (NOMA) has been widely studied in visible light communication (VLC) systems. As a main concern in NOMA-VLC systems, the power allocation scheme greatly affects the tradeoff between the total achievable data rate and user fairness. In this context, our main aim in this work was to find a more balanced power allocation scheme. To this end, an adaptive power allocation scheme based on multi-attribute decision making (MADM), which flexibly chooses between conventional power allocation or inverse power allocation (IPA) and the optimal power allocation factor, has been proposed. The concept of IPA is put forward for the first time and proves to be beneficial to achieving a higher total achievable data rate at the cost of user fairness. Moreover, considering users' mobility along certain trajectories, we derived a fitting model of the optimal power allocation factor. The feasibility of the proposed adaptive scheme was verified through simulation and the fitting model was approximated to be the sum of three Gaussian functions.

1. Introduction

Due to the ever-increasing penetration of wireless communication devices such as smartphones and tablets, rapidly growing wireless data traffic is expected to exceed 500 exabytes by 2020 [1], which is placing pressure on the dwindling radio frequency (RF) spectrum. Along with considerable advances in solid-state lighting, visible light communication (VLC) [2–4] supporting remarkably high-speed wireless communication has attracted great attention as a promising technology in applications such as the Internet of Things (IoT), 5G systems, underwater communications, vehicle-to-vehicle communication, and so on. In addition to the nature of its wide available bandwidth, VLC also features low power consumption, an unlicensed spectrum, enhanced confidentiality, and anti-electromagnetic interference, etc.

In VLC, it is essential to ensure the core functionality of providing multiple users with ubiquitous connectivity as well as broadband communication. To this effect, an appropriate multiple access (MA) scheme should be involved in dealing with simultaneous network access requests from multiple users. Traditionally, orthogonal multiple access (OMA) schemes have been applied to VLC systems, including carrier sense multiple access (CSMA), code division multiple access (CDMA), and orthogonal frequency division multiple access (OFDMA) [5]. Recently, a spectrum-efficient multiple access scheme called non-orthogonal multiple access (NOMA) has been proposed to further enhance system capacity and achieve a better balance between system fairness and throughput [6,7]. As a promising solution for next generation wireless networks, NOMA allocates different power levels to each user based on

its channel condition, thus achieving power-domain multiplexing of multiple users. Differently from a traditional OMA system, NOMA allow users to share all time-frequency (TF) resources and has proven to be superior theoretically and experimentally [8]. Apart from its applications in RF communications, NOMA has been introduced to VLC systems [9] and abundant research achievements have been obtained [10–13], especially those concerning power allocation schemes. In the literature by L. Yin et al. [14], the performance of NOMA-VLC was investigated based on a fixed power allocation (FPA) scheme. In addition, a channel-dependent gain ratio power allocation (GRPA) scheme was proposed in [9], which turned out to be superior to the FPA scheme. In addition, two types of quality of service (QoS) guaranteed power allocation have been proposed to iteratively optimize the sum user rate or max-min user rate utilizing gradient projection (GP) algorithm [15]. However, in all the existing works, users with a lower channel gain are always allocated a higher power level, which has been regarded as a basic principle in NOMA and has been proven to be beneficial to user fairness.

In our work, we begin with a hypothesis, which can be called inverse power allocation (IPA), that the total achievable data rate may be higher if users with a worse channel condition are allocated less power. We then prove this through theoretical formulas and simulation analysis. However, the total achievable data rate gain was obtained at a cost of user fairness. Hence, in order to achieve a better balance between total achievable data rate and user fairness, we attempted to find an adaptive power allocation scheme with which to combine conventional power allocation and IPA flexibly. To this effect, a multi-attribute decision making (MADM) algorithm was adopted to choose a suitable scheme, i.e., conventional or IPA, and an optimal power allocation factor in real time according to a mathematical comprehensive assessment of the total achievable data rate and user fairness. Moreover, by assuming users walk through certain trajectories within the optical attocell, we obtained a fitting model of the optimal power allocation factor utilizing the curve fitting technique.

The contribution of this paper is three-fold: first, to the best of our knowledge, this is the first work involving IPA in NOMA-VLC systems; second, an adaptive power allocation scheme based on MADM is proposed, which effectively combines IPA with conventional power allocation and facilitates the choice of an optimal power allocation factor; and, finally, taking users' mobility into account, a fitting model of optimal power allocation factor is presented.

The remainder of the paper is organized as follows: Section 2 illustates the model of the NOMA-VLC system. In Section 3, the IPA scheme is presented and the effect of it on system performance is discussed. An overall adaptive power allocation scheme is proposed in Section 4. In Section 5, the simulation results and discussion are presented. The modeling of the optimal power allocation factor for a mobile NOMA-VLC system is presented in Section 6. Finally, Section 7 concludes the paper.

2. System Model

Figure 1 shows the NOMA-VLC system model. All the devices were purchased from Vishay (Tianjin, China). For illustrative purposes, we consider a single optical attocell deployment and mainly focus on the NOMA downlink in an indoor environment, in which one light-emitting-diode (LED) transmitter is installed and M users are served. The LED transmitter can not only provide illumination but also convert electrical signals, which derive from a power line communications (PLC) backbone network, into optical signals by modulating the intensity of the emitted light. In addition, each user is equipped with a single photodiode (PD), which is used for extraction of the transmitted signal from the received optical carrier by direct detection. As is shown in Figure 1, R denotes the maximum cell radius, H denotes the vertical distance from the LED to the receiving plane of the users, and r_k denotes the horizontal separation from the k-th user to the LED.
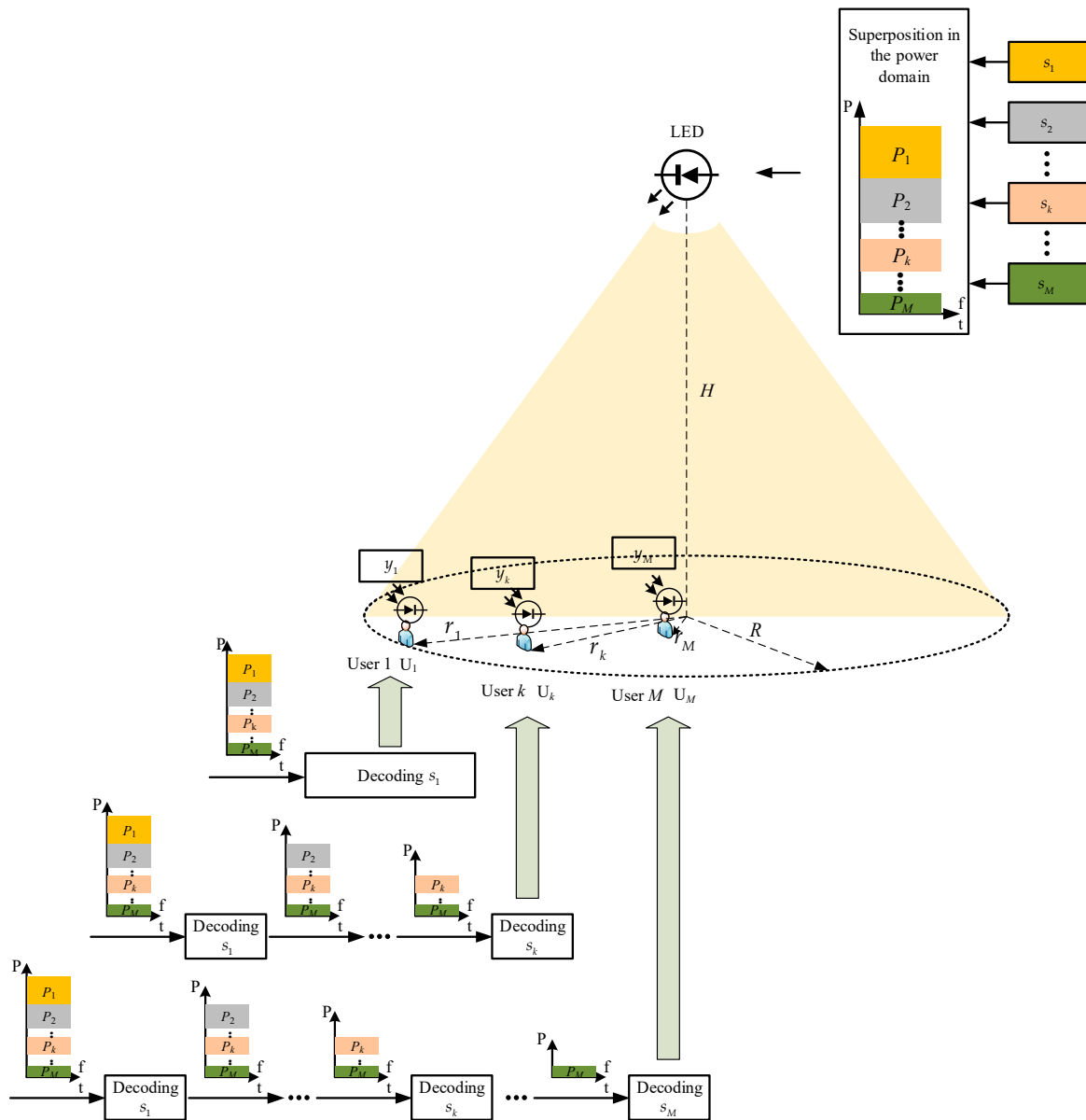
Figure 1. System model of non-orthogonal multiple access visible light communication (NOMA-VLC). Legend: LED, light-emitting-diode.

We assume that the LED follows a generalized Lambertian radiation pattern and the PD at each user faces vertically upwards with the width of the field of view denoted by ψ_{FOV}. Due to the weakness of diffuse components, which have proven to be at least 7 dB lower than the line of sight (LOS) component [16], the direct current (DC) channel gain for the k-th user can be approximately calculated by considering the LOS link, the wideband nature of VLC, and the shadowing effect:

$$
\begin{aligned}
h_k &= \frac{(m+1)AR_p}{2\pi d_k^2} \cos^m(\phi_k) \cos(\psi_k) T_s(\psi_k) g(\psi_k) \\
&= \frac{AR_p(m+1)H^{m+1} T_s(\psi_k) g(\psi_k)}{2\pi (r_k^2 + H^2)^{m+3/2}}
\end{aligned}, \tag{1}
$$

Here, m denotes the order of the Lambertian radiation pattern, which is derived from the semi-angle of the LED, $\Phi_{1/2}$, as $m = -1/\log_2(\cos(\Phi_{1/2}))$; A denotes the physical area of the PD; R_p denotes the responsivity of the PD; d_k denotes the Euclidean distance between the k-th user and the LED; ϕ_k denotes the angle of irradiance at the k-th user; ψ_k denotes the angle of incidence at the k-th

user; $T_s(\psi_k)$ denotes the gain of the optical filter used at the receiver; and $g(\psi_k)$ denotes the gain of the optical concentrator used at the receiver front-end, which is given by [17]

$$g(\psi_k) = \begin{cases} \frac{n^2}{\sin^2 \psi_{FOV}} & 0 \leq \varphi_k \leq \psi_{FOV} \\ 0 & \varphi_k \geq \psi_{FOV}, \end{cases} \tag{2}$$

where n denotes the refractive index of the optical concentrator.

Without loss of generality, based on the DC channel gains, all users $U_1, \cdots, U_M$ can be sorted in an ascending order as $h_1 \leq \cdots \leq h_k \leq \cdots \leq h_M$.

The principle of NOMA is also illustrated in Figure 1. At the transmitter side, the messages $\{s_i, i = 1, 2, \cdots M\}$ intended for all the corresponding users are superposed in the power domain with associated power values $\{P_i, i = 1, 2, \cdots M\}$ and then transmitted simultaneously as

$$x = \sum_{i=1}^{M} a_i \sqrt{P_{elec}} s_i + I_{DC}, \tag{3}$$

where x denotes the superposed signal of $\{s_i, i = 1, 2, \cdots M\}$; P_{elec} denotes the total electrical power of all the message signals; I_{DC} denotes a DC bias added before transmission to ensure the positive signal; and a_i denotes the power allocation coefficient for the i-th user, which should satisfy the following two conditions: $\sum_{i=1}^{M} a_i^2 = 1$, according to the total power constraint; and $a_1 \geq \cdots \geq a_k \geq \cdots \geq a_M$, according to the basic principle of conventional NOMA.

Similarly to the power allocation coefficient, another equivalent parameter, the power allocation factor α, can be defined as $\alpha = a_i^2 / a_{i-1}^2, i = 2, \cdots M$, which can be constant or variable along with i according to different power allocation schemes, i.e., FPA or GRPA.

At the receiver side of the k-th user, taking the DC channel gain and the additive white Gaussian noise (AWGN) into account and removing the DC term, we can obtain the received signal

$$y_k = \sqrt{P_{elec}} h_k (\sum_{i=1}^{M} a_i s_i) + z_k, \tag{4}$$

where y_k denotes the received signal at the k-th user and z_k denotes the AWGN with a zero mean and variance σ_k^2. Moreover, $\sigma_k^2 = N_0 B$, where N_0 denotes the noise power spectral density and B denotes the channel bandwidth. Next, the successive interference cancellation (SIC) is performed to extract s_k from the received signal, with the process being as follows: first, we attempt to obtain the message signal s_1 intended for the first user, with the other signals treated as noise; then, by subtracting s_1 from the received signal, with the residual interference fraction denoted by ε [18], and treating the message signal for the users with stronger channel gains than the second user as noise, we can obtain the message signal s_2; and finally, by following the former method, $s_3, \cdots, s_{k-1}, s_k$ are obtained in sequence. According to the Shannon Theorem, the achievable data rate for the k-th user may be given by

$$R_k = \begin{cases} \frac{B}{2} \log_2 (1 + \frac{(h_k a_k)^2}{\sum_{i=1}^{k-1} \varepsilon (h_k a_i)^2 + \sum_{j=k+1}^{M} (h_k a_j)^2 + 1/\rho}) & k = 1, \cdots, M-1 \\ \frac{B}{2} \log_2 (1 + \frac{(h_k a_k)^2}{\sum_{i=1}^{k-1} \varepsilon (h_k a_i)^2 + 1/\rho}) & k = M \end{cases}, \tag{5}$$

where $\rho = P_{elec} / (N_0 B)$ and the scaling factor $1/2$ comes from the constraint of the real-valued signal, i.e., Hermitian symmetry.

3. Inverse Power Allocation Scheme

We define the features of an IPA scheme as follows: first, at the transmitter side, users with a worse channel condition are allocated less power, and second, at the receiver side, the message signal intended for users with a worse channel condition has a higher decoding order. The differences and links between the IPA scheme and the conventional power allocation scheme are illustrated in Figure 2, in which we assume that there are two users for simplicity, i.e., $M = 2$.

Let a_i, a_i denote the power allocation coefficient for user i in the conventional power allocation case and the IPA case, respectively, where $i = 1, 2$. As mentioned above, $a_1 \geq a_2$, $a_1^2 + a_2^2 = 1$, $a_1' \leq a_2'$, and $a_1'^2 + a_2'^2 = 1$. In addition, the power allocation factor α, which should be less than 1, can be described as a_2^2/a_1^2 or $a_1'^2/a_2'^2$ in the conventional power allocation case or the IPA case, respectively. Moreover, Equations (6) and (7) can be easily derived for the below two cases.

$$
\begin{cases}
a_1^2 = \frac{1}{1+\alpha} \\
a_2^2 = \frac{\alpha}{1+\alpha},
\end{cases}
\tag{6}
$$

$$
\begin{cases}
a_1'^2 = \frac{\alpha}{1+\alpha} \\
a_2'^2 = \frac{1}{1+\alpha}.
\end{cases}
\tag{7}
$$

According to Equations (5) and (6), the total achievable data rate of the two users in the conventional power allocation case can be given by:

$$
\begin{aligned}
R_{\text{total}} &= \frac{B}{2} \log_2\left(1 + \frac{(h_1 a_1)^2}{(h_1 a_2)^2 + 1/\rho}\right) + \frac{B}{2} \log_2\left(1 + \frac{(h_2 a_2)^2}{\varepsilon (h_2 a_1)^2 + 1/\rho}\right) \\
&= \frac{B}{2} \log_2\left[\left(1 + \frac{(h_1 a_1)^2}{(h_1 a_2)^2 + 1/\rho}\right)\left(1 + \frac{(h_2 a_2)^2}{\varepsilon (h_2 a_1)^2 + 1/\rho}\right)\right] \\
&= \frac{B}{2} \log_2\left[\left(1 + \frac{h_1^2}{h_1^2 \alpha + (\alpha+1)/\rho}\right)\left(1 + \frac{h_2^2 \alpha}{\varepsilon h_2^2 + (\alpha+1)/\rho}\right)\right]
\end{aligned}
\tag{8}
$$

Similarly, the total achievable data rate of the two users in the IPA case can be given by:

$$
\begin{aligned}
R'_{\text{total}} &= \frac{B}{2} \log_2\left(1 + \frac{(h_1 a_1')^2}{\varepsilon (h_1 a_2')^2 + 1/\rho}\right) + \frac{B}{2} \log_2\left(1 + \frac{(h_2 a_2')^2}{(h_2 a_1')^2 + 1/\rho}\right) \\
&= \frac{B}{2} \log_2\left[\left(1 + \frac{(h_1 a_1')^2}{\varepsilon (h_1 a_2')^2 + 1/\rho}\right)\left(1 + \frac{(h_2 a_2')^2}{(h_2 a_1')^2 + 1/\rho}\right)\right] \\
&= \frac{B}{2} \log_2\left[\left(1 + \frac{h_1^2 \alpha}{\varepsilon h_1^2 + (\alpha+1)/\rho}\right)\left(1 + \frac{h_2^2}{h_2^2 \alpha + (\alpha+1)/\rho}\right)\right]
\end{aligned}
\tag{9}
$$

Next, we carry out a numerical simulation utilizing MATLAB R2016a to intuitively show the size relationship of the total achievable data rate in these two cases; the simulation setup is parameterized as Table 1. In this setup, the PD parameters are set according to BPW21R [19], a planar Silicon PN photodiode in a hermetically sealed short TO-5 case. In addition, the simulation step of the horizontal separation from each user to the LED, i.e., r_1 and r_2, is set to 0.1 m. In accordance with [9], we chose $\alpha = 0.3$ and $\alpha = 0.4$, which have been proven to be optimal to achieving the best performance when an FPA scheme is adopted. Figure 3 shows the simulation results.

As is shown in Figure 3, the IPA scheme leads to a higher total achievable data rate compared with the conventional power allocation scheme whether $\alpha = 0.3$ or $\alpha = 0.4$, and the gain increases with a decrease in α. However, it is obvious that the IPA scheme will cause serious unfairness between the two users. Hence, adopting the IPA scheme solely for the NOMA-VLC system is not optimal; this encouraged us to propose an adaptive power allocation scheme to achieve a better balance between total achievable data rate and user fairness by choosing a suitable scheme, i.e., conventional or inverse, and an optimal power allocation factor.
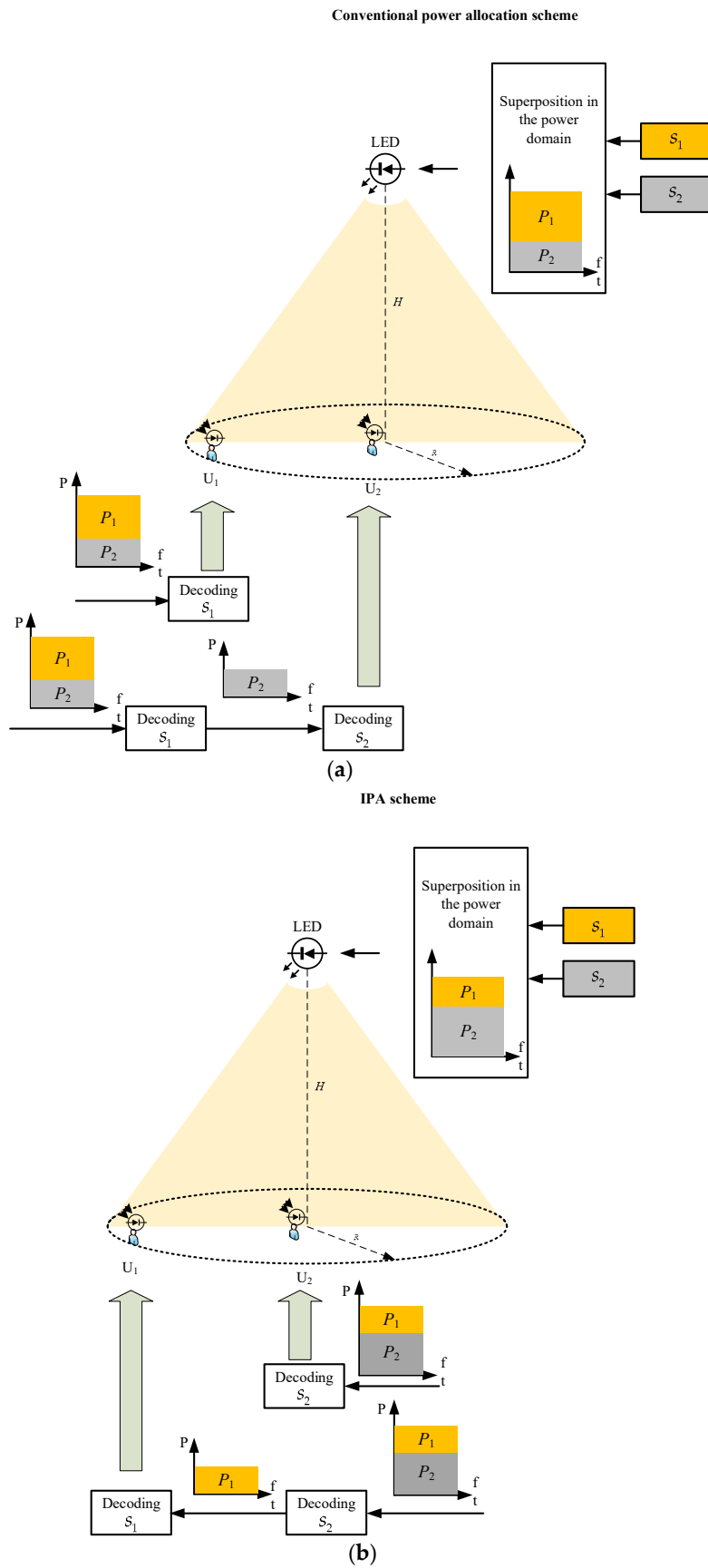
Conventional power allocation scheme

IPA scheme

Figure 2. NOMA-VLC system based on different power allocation schemes: (**a**) conventional power allocation scheme; (**b**) inverse power allocation (IPA) scheme.

Table 1. Simulation parameters. Legend: PD, photodiode.

Parameter Name, Notation	Value
Vertical height, H	3 m
LED semi-angle, $\Phi_{1/2}$	60°
Signal power, P_{elec}	1.25 mW
Channel bandwidth, B	20 MHz
Noise power spectral density, N_0	10^{-21} A^2/Hz
PD physical area, A	7.5 mm^2
PD responsivity, R_p	0.48 A/W
PD's field of view (FOV), ψ_{FOV}	50°
Optical filter gain, $T_s(\psi_k)$	1
Refractive index, n	1.5
Power allocation factor, α	0.3
Residual interference fraction, ε	0.1

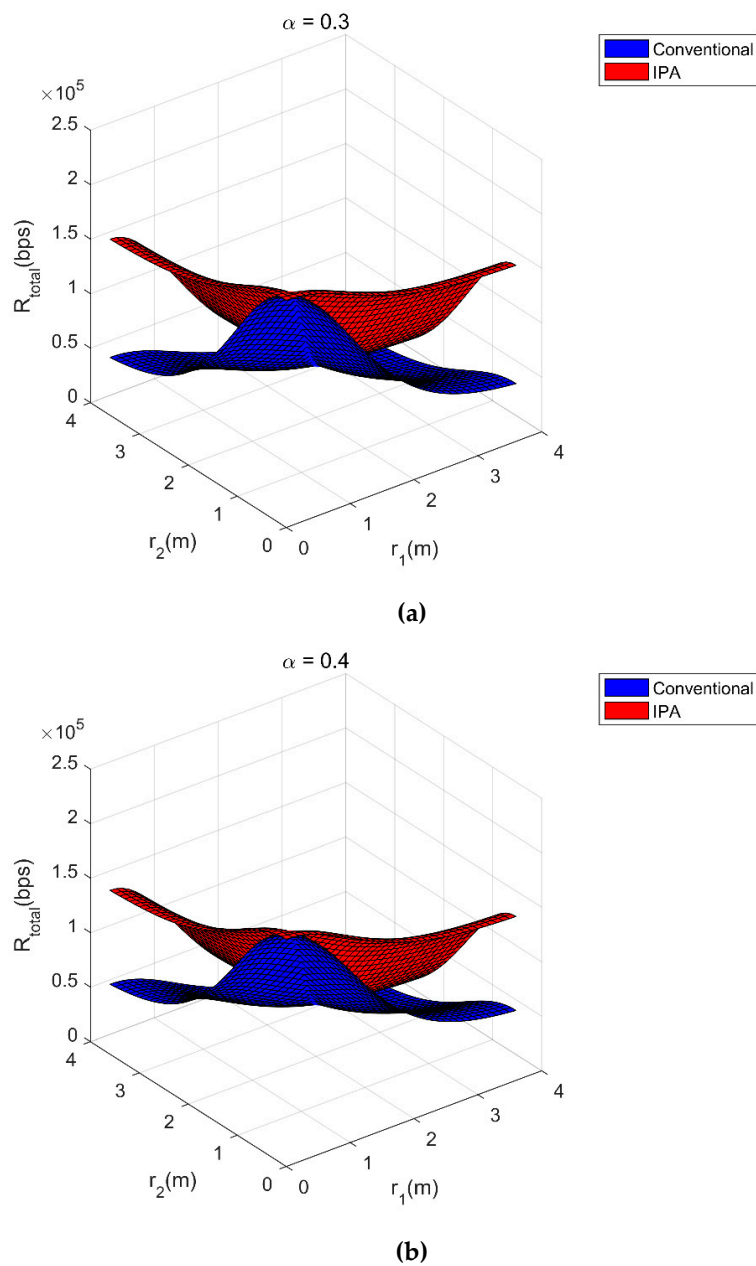

(a)

(b)

Figure 3. Total achievable data rate in conventional power allocation case and IPA case when: (**a**) $\alpha = 0.3$; (**b**) $\alpha = 0.4$.

4. Adaptive Power Allocation Scheme

In this section, we propose an adaptive power allocation scheme based on MADM, wherein the total achievable data rate and user fairness are selected as decision parameters. Our goal was to choose the most appropriate combination of a power allocation scheme and corresponding power allocation factor, and the change in users' location. Moreover, the choice space is a $u \times v$ matrix, where u is the number of candidate schemes, i.e., $u = 2$, and v is the number of candidate power allocation factors, which are discretized artificially. The concrete implementation process is as follows: first, the standard deviation method [20], which uses mathematical variance information to solve the MADM problem, is used to obtain the objective weight of each decision parameter; then, the technique for order preference by similarity to the ideal solution (TOPSIS) [21], which makes the most of the information of the raw data, is used to sort the candidate combinations in order to choose the best one.

According to the standard deviation method, the main steps used to obtain the objective weight of each decision parameter are as follows:

First, the normalized decision matrix C is constructed as

$$
C = \begin{pmatrix} C_{11} & C_{12} \\ C_{21} & C_{22} \\ \dots & \dots \\ \dots & \dots \\ C_{p1} & C_{p2} \end{pmatrix},
\tag{10}
$$

where p is the total number of candidate combinations and $p = u \times v = 2v$, and elements C_{k1}, C_{k2} are the normalized values of total achievable data rate and user fairness, respectively, when the k-th candidate combination is chosen. As for the benefit parameters, their normalization can be given by [22]

$$
C_{ki} = \frac{S_{ki} - \min(S_{xi}, 1 \le x \le p)}{\max(S_{xi}, 1 \le x \le p) - \min(S_{xi}, 1 \le x \le p)}, \quad 1 \le k \le p, i = 1,2,
\tag{11}
$$

where S_{k1} is the value of the total achievable data rate when the k-th candidate combination is chosen, which can be calculated as Equations (8) and (9), and S_{k2} is the value of user fairness when the k-th candidate combination is chosen, which can be given by

$$
S_{k2} = \frac{\min(R_1|k, R_2|k)}{\max(R_1|k, R_2|k)}
$$

$$
= \begin{cases} \dfrac{\min(\frac{B}{2}\log_2(1+\frac{h_1{}^2}{h_1{}^2\alpha+(\alpha+1)/\rho}), \frac{B}{2}\log_2(1+\frac{h_2{}^2\alpha}{\varepsilon h_2{}^2+(\alpha+1)/\rho}))}{\max(\frac{B}{2}\log_2(1+\frac{h_1{}^2}{h_1{}^2\alpha+(\alpha+1)/\rho}), \frac{B}{2}\log_2(1+\frac{h_2{}^2\alpha}{\varepsilon h_2{}^2+(\alpha+1)/\rho}))}, \\ \qquad k \le p/2, r_1 \ge r_2, or\, k > p/2, r_1 \le r_2 \\[6pt] \dfrac{\min(\frac{B}{2}\log_2(1+\frac{h_1{}^2\alpha}{\varepsilon h_1{}^2+(\alpha+1)/\rho}), \frac{B}{2}\log_2(1+\frac{h_2{}^2}{h_2{}^2\alpha+(\alpha+1)/\rho}))}{\max(\frac{B}{2}\log_2(1+\frac{h_1{}^2\alpha}{\varepsilon h_1{}^2+(\alpha+1)/\rho}), \frac{B}{2}\log_2(1+\frac{h_2{}^2}{h_2{}^2\alpha+(\alpha+1)/\rho}))}, \\ \qquad k \le p/2, r_1 \le r_2, or\, k > p/2, r_1 \ge r_2, \end{cases}
\tag{12}
$$

where $R_1|k$, $R_2|k$ is the achievable data rate of User 1 and User 2, respectively, when the k-th candidate combination is chosen.

Second, the objective weight of each decision parameter is calculated as

$$
w_j = \frac{\sqrt{\sum\limits_{i=1}^{p} \left(C_{ij} - \frac{1}{p}\sum\limits_{i=1}^{p} C_{ij}\right)^2 /(p-1)}}{\sum\limits_{j=1}^{2} \sqrt{\sum\limits_{i=1}^{p} \left(C_{ij} - \frac{1}{p}\sum\limits_{i=1}^{p} C_{ij}\right)^2 /(p-1)}}, \quad j = 1,2,
\tag{13}
$$

where w_1, w_2, are the objective weights of the total achievable data rate and user fairness, respectively.

Once we obtain the objective weight of each parameter, according to TOPSIS, the main steps which must be used to choose the best candidate combination are as follows:

1. Construct the weighted normalized decision matrix D as:

$$D = \begin{pmatrix} D_{11} & D_{12} \\ D_{21} & D_{22} \\ \cdots & \cdots \\ \cdots & \cdots \\ D_{p1} & D_{p2} \end{pmatrix} = \begin{pmatrix} w_1 C_{11} & w_2 C_{12} \\ w_1 C_{21} & w_2 C_{22} \\ \cdots & \cdots \\ \cdots & \cdots \\ w_1 C_{p1} & w_2 C_{p2} \end{pmatrix} \tag{14}$$

2. Determine the positive ideal solution matrix Y^+ as:

$$Y^+ = \begin{pmatrix} Y_1^+ & Y_2^+ \end{pmatrix} = \begin{pmatrix} \max_k (D_{k1}) & \max_k (D_{k2}) \end{pmatrix}, \quad k = 1, 2, \cdots, p. \tag{15}$$

3. Determine the negative ideal solution matrix Y^- as:

$$Y^- = \begin{pmatrix} Y_1^- & Y_2^- \end{pmatrix} = \begin{pmatrix} \min_k (D_{k1}) & \min_k (D_{k2}) \end{pmatrix}, \quad k = 1, 2, \cdots, p. \tag{16}$$

4. Calculate the Euclidean distance between each solution and the positive ideal solution as:

$$F_k^+ = \sqrt{\sum_{i=1}^{2} (D_{ki} - Y_i^+)^2}, \quad k = 1, 2, \cdots, p. \tag{17}$$

5. Calculate the Euclidean distance between each solution and the negative ideal solution as:

$$F_k^- = \sqrt{\sum_{i=1}^{2} (D_{ki} - Y_i^-)^2}, \quad k = 1, 2, \cdots, p. \tag{18}$$

6. Calculate the relative proximity of each solution to the ideal solution as:

$$G_k = \frac{F_k^-}{F_k^+ + F_k^-}, \quad 0 \le G_k \le 1, k = 1, 2, \cdots, p. \tag{19}$$

7. Find the best combination of a power allocation scheme and the corresponding power allocation factor by:

$$\underset{k}{\operatorname{argmax}} G_k, \quad k = 1, 2, \cdots, p. \tag{20}$$

Next, we extend the adaptive power allocation scheme to adapt to more realistic scenarios in which M users exist and $M > 2$. For ease of identification, we further define $\alpha_{(i-1)i}$ to describe the power allocation factor between the $(i-1)$-th user and the i-th one. As mentioned before, $\alpha_{(i-1)i}$ can be expressed as $\alpha_{(i-1)i} = a_i^2 / a_{i-1}^2, i = 2, \cdots M$. The concrete process with which to obtain the optimal $\alpha_{(i-1)i}, i = 2, \cdots M$ is presented below.

First, we use α_{12}, which is now a variable to be optimized, to express all the other power allocation factors, namely, $\alpha_{23}, \cdots, \alpha_{(M-1)M}$. According to GRPA, $\alpha_{(i-1)i} = (h_1/h_i)^i, i = 2, \cdots, M$. Based on this equation, it is easy to obtain the recursion relation of the power allocation factor: $\alpha_{i(i+1)}/\alpha_{(i-1)i} = h_1 h_i^i / h_{i+1}^{i+1}, i = 2, \cdots, M$. Following this recursion relation, we can easily express $\alpha_{23}, \cdots, \alpha_{(M-1)M}$ in terms of α_{12}. Next, we obtain the optimal α_{12} by means of the proposed adaptive scheme, in which the Equations (8), (9) and (12) need to be extended to take the effect of all users on the decision parameters,

namely, the total achievable data rate and user fairness, into account. Specifically, Equations (8), (9) and (12) are extended as Equations (21)–(23), respectively.

$$
\begin{aligned}
R_{\text{total}} &= \sum_{k=1}^{M} R_k \\
&= \frac{B}{2} \log_2 \left(1 + \frac{(h_M a_M)^2}{\sum_{i=1}^{M-1} \varepsilon (h_M a_i)^2 + 1/\rho}\right) + \sum_{k=1}^{M-1} \frac{B}{2} \log_2 \left(1 + \frac{(h_k a_k)^2}{\sum_{i=1}^{k-1} \varepsilon (h_k a_i)^2 + \sum_{j=k+1}^{M} (h_k a_j)^2 + 1/\rho}\right),
\end{aligned}
\tag{21}
$$

$$
\begin{aligned}
R'_{\text{total}} &= \sum_{k=1}^{M} R'_k \\
&= \frac{B}{2} \log_2 \left(1 + \frac{(h_1 a'_1)^2}{\sum_{i=2}^{M} \varepsilon (h_1 a'_i)^2 + 1/\rho}\right) + \sum_{k=2}^{M} \frac{B}{2} \log_2 \left(1 + \frac{(h_k a'_k)^2}{\sum_{i=k+1}^{M} \varepsilon (h_k a'_i)^2 + \sum_{j=1}^{k-1} (h_k a'_j)^2 + 1/\rho}\right),
\end{aligned}
\tag{22}
$$

$$
S_{k2} = \frac{\min(R_1|k, R_2|k, \cdots, R_M|k)}{\max(R_1|k, R_2|k \cdots, R_M|k)} \ or \ \frac{\min(R'_1|k, R'_2|k, \cdots, R'_M|k)}{\max(R'_1|k, R'_2|k \cdots, R'_M|k)}, \ Conventional \ or \ IPA,
\tag{23}
$$

where a_k, a'_k can be expressed as follows:

$$
a_k = \begin{cases} \sqrt{1/(1 + \alpha_{12} + \alpha_{12} \times \alpha_{23} + \cdots + \alpha_{12} \times \alpha_{23} \times \cdots \times \alpha_{(M-1)M})} & ,k = 1 \\ \sqrt{\alpha_{12} \times \alpha_{23} \times \cdots \times \alpha_{(k-1)k}/(1 + \alpha_{12} + \alpha_{12} \times \alpha_{23} + \cdots + \alpha_{12} \times \alpha_{23} \times \cdots \times \alpha_{(M-1)M})} & ,k = 2, \cdots, M \end{cases}
\tag{24}
$$

$$
a'_k = \begin{cases} \sqrt{1/(1 + \alpha_{(M-1)M} + \alpha_{(M-1)M} \times \alpha_{(M-2)(M-1)} + \cdots + \alpha_{12} \times \alpha_{23} \times \cdots \times \alpha_{(M-1)M})} \\ \quad ,k = M \\ \sqrt{\alpha_{k(k+1)} \times \cdots \times \alpha_{(M-1)M}/(1 + \alpha_{(M-1)M} + \alpha_{(M-1)M} \times \alpha_{(M-2)(M-1)} + \cdots + \alpha_{12} \times \alpha_{23} \times \cdots \times \alpha_{(M-1)M})} \\ \quad ,k = 1, \cdots, M-1. \end{cases}
\tag{25}
$$

Substituting the expressions of $\alpha_{23}, \cdots, \alpha_{(M-1)M}$ into (24) and (25), we can also obtain a_k, a'_k in terms of α_{12}. Finally, once the optimal α_{12} is obtained, we can easily determine the optimal $\alpha_{23}, \cdots, \alpha_{(M-1)M}$ in turn.

In order to make the proposed adaptive power allocation scheme clearer, a flow chart of the specific implementation process is given in Figure 4.
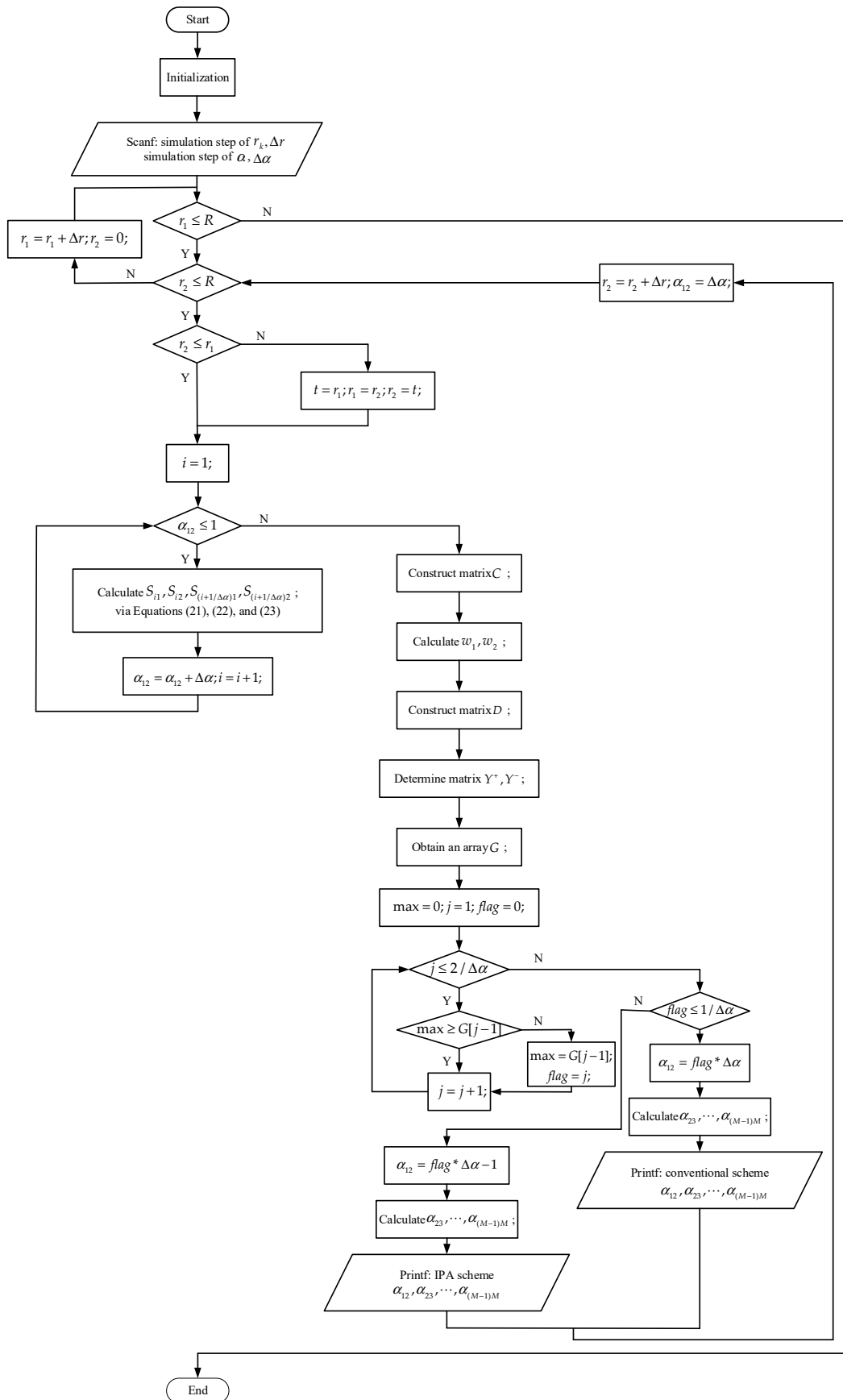
Figure 4. Flow chart of the proposed adaptive power allocation scheme.

5. Simulation Results and Discussion

In order to verify the feasibility of our proposed adaptive power allocation scheme, we conducted a simulation analysis utilizing matrix laboratory (MATLAB) R2016a, and three scenarios were chosen as examples: Scenario 1, $M = 2$; Scenario 2, $M = 5$; and Scenario 3, $M = 10$. In addition, the simulation step r_k was still set to 0.1 m and the simulation step of α was set to 0.01. Other parameters were the same as in Table 1. Moreover, we also simulated these three scenarios with a GRPA scheme and IPA scheme, respectively, in order to verify the superiority of our proposed scheme compared with them. For Scenario 1, the simulation results are shown in Figure 5 with the ergodic positions of both users taken into account. For Scenario 2 and Scenario 3, we randomly chose the combination of positions of all users involved and tested each scheme ten times, with the simulation results shown in Figures 6 and 7.

(a)

(b)
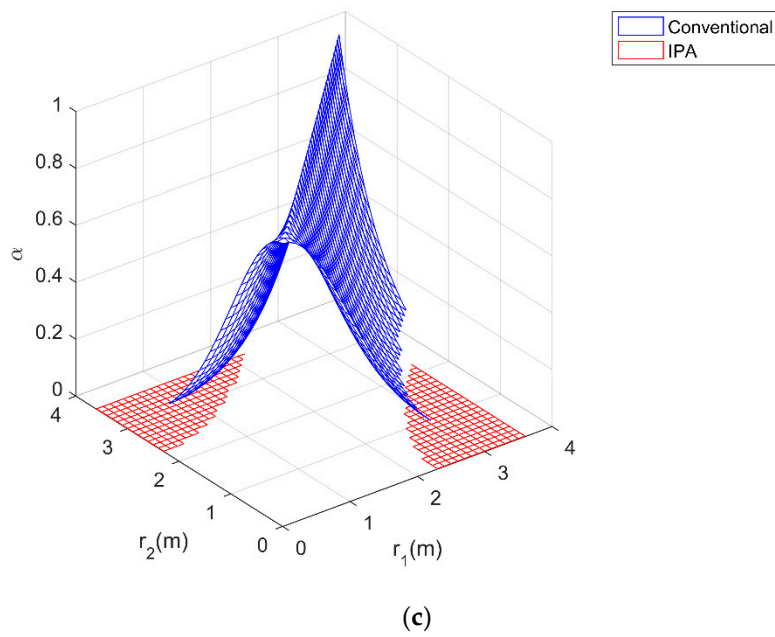
Figure 5. *Cont.*

(**c**)
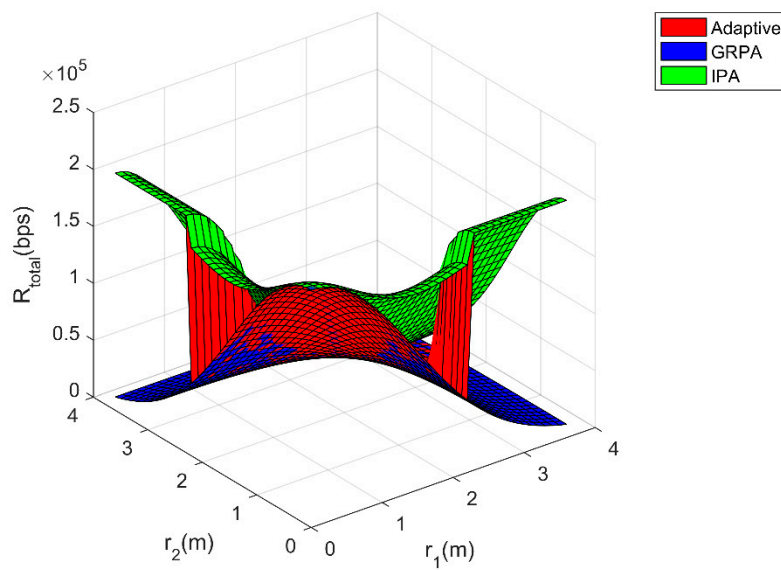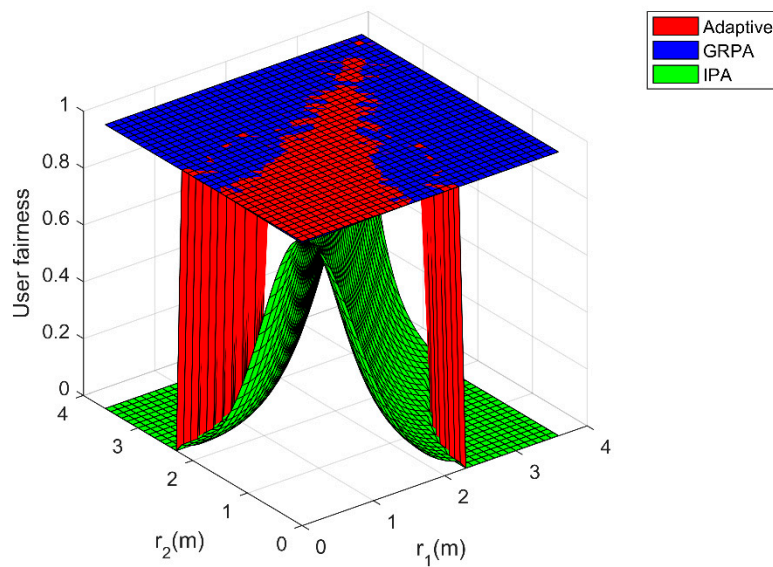
Figure 5. Simulation results for Scenario 1 based on the proposed adaptive power allocation scheme, gain ratio power allocation (GRPA) scheme, and IPA scheme, respectively: (**a**) total achievable data rate; (**b**) user fairness; (**c**) optimal power allocation factor.
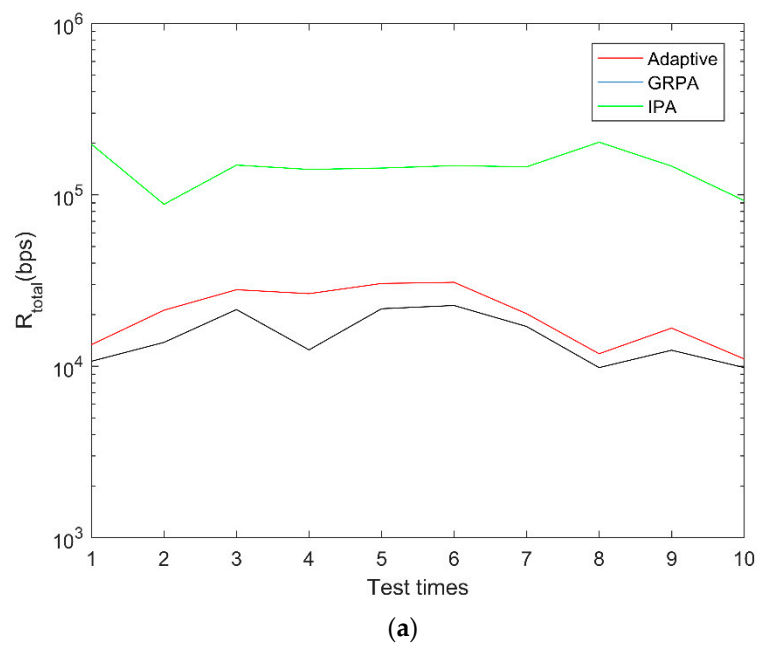

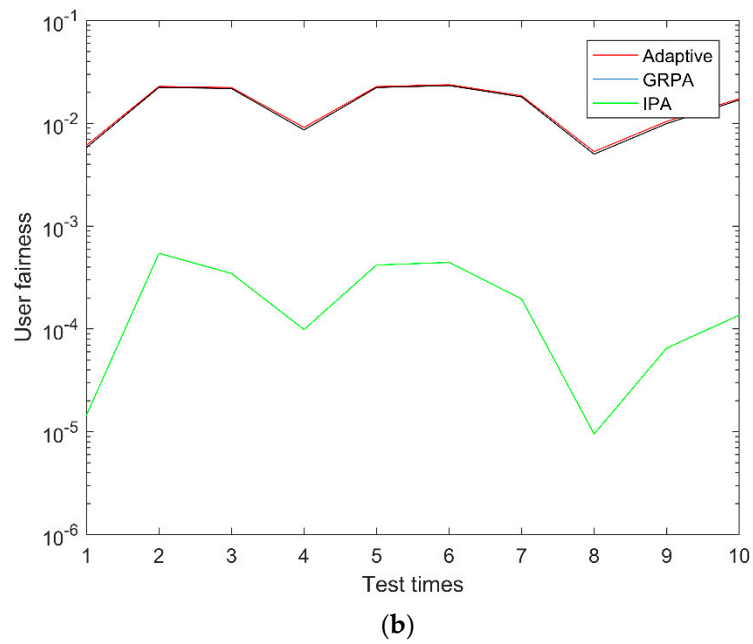(**a**)

Figure 6. *Cont.*

(**b**)

Figure 6. Simulation results for Scenario 2 based on the proposed adaptive power allocation scheme, GRPA scheme, and IPA scheme, respectively, wherein the randomly generated combinations of $r_1, r_2, \cdots, r_5$ for the 10 tests are (3.5309, 2.8755, 2.2167, 0.5458, 0.3096), (3.4397, 2.4176, 2.3547, 1.6103, 1.4316), (3.0480, 2.3202, 1.7318, 1.3096, 0.8124), (3.5805, 2.1633, 2.1595, 1.9316, 0.9357), (3.0654, 2.2295, 1.4686, 1.4371, 0.8664), (3.0212, 2.2223, 1.5741, 1.1445, 0.8263), (3.1828, 2.5616, 2.4763, 2.1451, 0.8921), (3.5729, 2.9899, 2.1466, 0.7575, 0.1092), (3.4661, 2.6299, 2.5681, 1.3844, 0.8624), and (3.5628, 3.0949, 2.8034, 2.5635, 1.4087), respectively: (**a**) total achievable data rate; (**b**) user fairness.
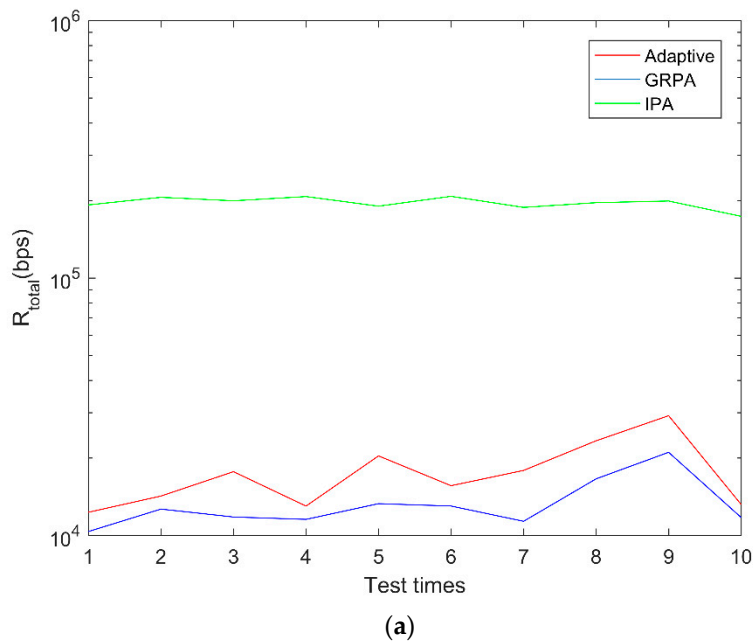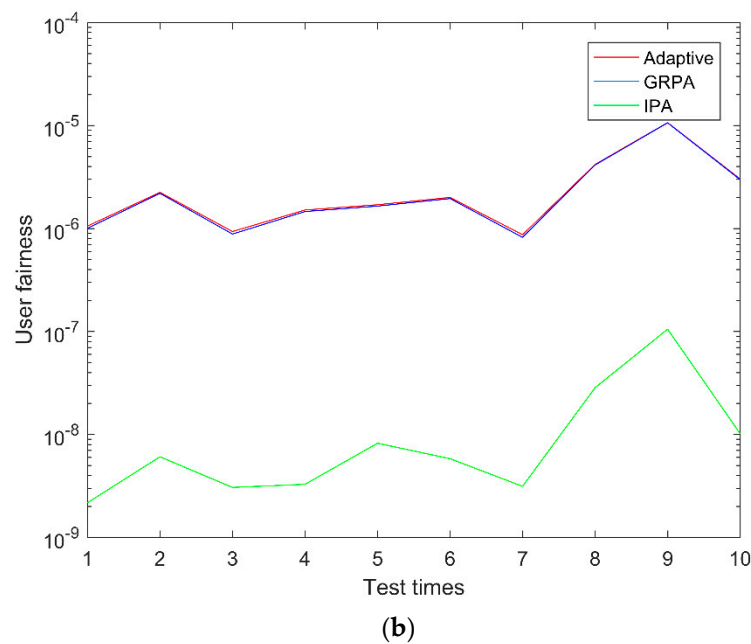

(**a**)

Figure 7. *Cont.*

(b)

Figure 7. Simulation results for Scenario 3 based on the proposed adaptive power allocation scheme, GRPA scheme, and IPA scheme, respectively, wherein the randomly generated combinations of $r_1, r_2, \cdots, r_{10}$ for the 10 tests are (3.5635, 2.9895, 2.6482, 2.2378, 2.1181, 1.2470, 1.0532, 0.9620, 0.9131, 0.3908), (3.3684, 2.9048, 2.6485, 2.0980, 1.7719, 1.6640, 0.9519, 0.8605, 0.3101, 0.1060), (3.5600, 2.5837, 2.4566, 2.1188, 1.6979, 1.6005, 1.0897, 0.9554, 0.6994, 0.2629), (3.4459, 2.9862, 2.5604, 2.5197, 1.1499, 1.0042, 0.3522, 0.1674, 0.1249, 0.1154), (3.4804, 2.4649, 2.3756, 2.1224, 1.8073, 1.2344, 1.0010, 0.8116, 0.5897, 0.4315), (3.3871, 2.8256, 2.0628, 1.9249, 1.7022, 1.2225, 0.4711, 0.2751, 0.1956, 0.0432), (3.6230, 2.5424, 2.5316, 2.4171, 2.4164, 1.9551, 1.0932, 0.6460, 0.6205, 0.4642), (3.2883, 2.3745, 2.3405, 2.1248, 1.4024, 1.0412, 0.6931, 0.4675, 0.4042, 0.3604), (3.0934, 2.2558, 1.8612, 1.4571, 1.2727, 0.8702, 0.8700, 0.6669, 0.4472, 0.2755), and (3.4347, 2.9254, 2.8023, 2.7768, 2.0362, 1.7961, 1.4943, 1.2546, 1.0903, 0.6240), respectively: (**a**) total achievable data rate; (**b**) user fairness.

For Scenario 1, with regard to the proposed adaptive power allocation scheme, we can conclude from Figure 5a,b that when the distance between the two users is large enough, namely, when one is near the center of the optical attocell and the other one is near the edge, the total achievable data rate approaches a maximum of about 2.5×10^5 bps and the user fairness approaches a minimum of about zero. This is because the IPA scheme, which corresponds to the red region illustrated in Figure 5c, is adopted in this case. Note that this case is less common than the one in which the conventional power allocation scheme is adopted and that the value of the total achievable data rate and user fairness varies smoothly between 0.3×10^5 bps and 1.2×10^5 bps, and between 0.9 and 1, respectively. In addition, when comparing the proposed scheme with the GRPA scheme, we find that the total achievable data rate increases greatly at a small cost of user fairness; when comparing the proposed scheme with the IPA scheme, we find that the user fairness is improved greatly at a small cost of total achievable data rate. Specifically, when the proposed scheme, GRPA scheme, and IPA scheme are adopted, the mean values of the total achievable data rate are 9.7748×10^4 bps, 5.8142×10^4 bps, and 1.1455×10^5 bps, respectively, and the mean values of user fairness are 0.6913, 0.9989, and 0.2382, respectively. Apparently, the total achievable data rate gain of the proposed scheme reaches 68.2% compared to that of the GRPA scheme, while user fairness is reduced by only 30.8%; the user fairness gain of the proposed scheme reaches 190.2% compared with that of the IPA scheme, while the total achievable data rate is reduced by only 14.7%. Hence, we can conclude that the proposed adaptive scheme facilitates a better balance between total achievable data rate and user fairness. Moreover, from Figure 5c, we find that no matter which power allocation scheme is adopted, the optimal power allocation factor follows these two rules: first, the optimal power allocation factor increases with

decreasing distance between the two users; and second, when the distance between the two users remains unchanged, the optimal power allocation factor increases with an increase in the mean r_1 and r_2.

For Scenario 2, by considering Figure 6, we can easily obtain the mean values of the total achievable data rate and user fairness based on the three schemes. Specifically, compared with the GRPA scheme, the proposed scheme increases the total achievable data rate by about 38.51% at no cost of user fairness; compared with the IPA scheme, the proposed scheme increases the user fairness by a factor of 66.6750 and reduces the total achievable data rate by only 0.8556. Similarly, for Scenario 3, we can conclude from Figure 7 that the proposed scheme increases the total achievable data rate by about 32.54% at no cost of user fairness compared with the GRPA scheme and improves the user fairness by a factor of 156.6884 with a 90.97% loss of the total achievable data rate compared with the IPA scheme. When considering Figures 5–7 comprehensively, we find that the performance gain of the proposed scheme is relatively considerable, even with the increase in the number of users. The feasibility and superiority of our proposed adaptive scheme is verified accordingly.

It should be emphasized that our proposed adaptive power allocation scheme is not only suitable for the situation in which the IPA scheme is involved. If we aim to perform NOMA without sacrificing user fairness, that is to say, if only the conventional power allocation scheme is considered, our proposed adaptive scheme can also play a significant role in exploring the optimal power allocation factor based on the real time location of users and the MADM algorithm.

6. Modeling of Optimal Power Allocation Factor for Mobile NOMA-VLC

In order to further study the change rule of the optimal power allocation factor for mobile NOMA-VLC systems, we consider a mobile scenario, as shown in Figure 8, and establish the fitting model of the optimal power allocation factor in that case, in which two users walk along Trajectory 1 and Trajectory 2, respectively, with the same velocity (see Figure 8 for blue and red lines). Other parameters are the same as in Table 1.
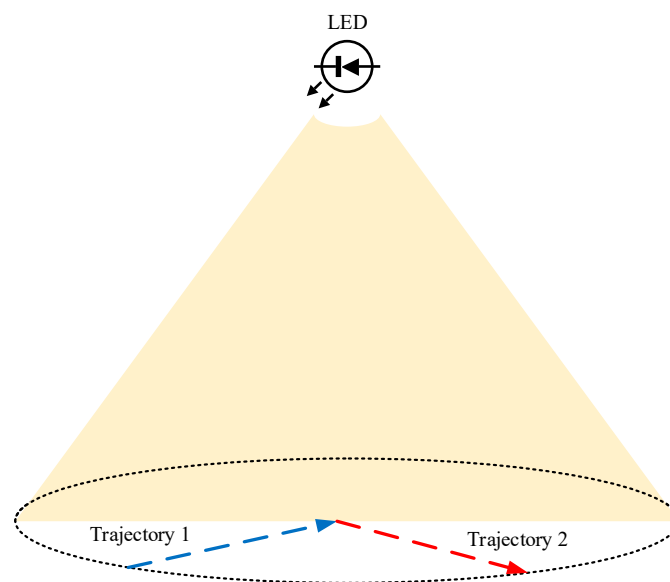

Figure 8. Movement trajectories of User 1 and User 2.

Based on our proposed adaptive power allocation scheme, we first obtain the optimal power allocation factor along with the movement distance of the two users, in which the simulation step is still set to 0.1 m. Then, we apply curve fitting techniques to establish the fitting model, in which the "leave-one-out cross-validation (LOOCV)" method [23] is adopted to avoid over-fitting. Specifically, we take four functions into account for curve fitting, i.e., exponential, Fourier, Gaussian, and sinusoidal.

In addition, in order to guarantee the conciseness and effectiveness of the fitting model, we limit the number of its terms to three or less, thus yielding 12 tests. Moreover, a nonlinear least squares (NLS) method is adopted due to its intrinsic capability to fit a large range of functions and to produce good estimates of the unknown parameters from small data sets. Based on a trust-region algorithm, this method tries to refine the parameters by iterative optimization, and we set the maximum number of iterations to 400. In the process, we used the root mean square error (RMSE) and R-square to assess the fitting accuracy; a better fitting model possesses a smaller value of RMSE and a value of R-square closer to 1. The best curve fitting is illustrated in Figure 9, and the corresponding RMSE value and R-square value are 0.01627 and 0.9953, respectively.
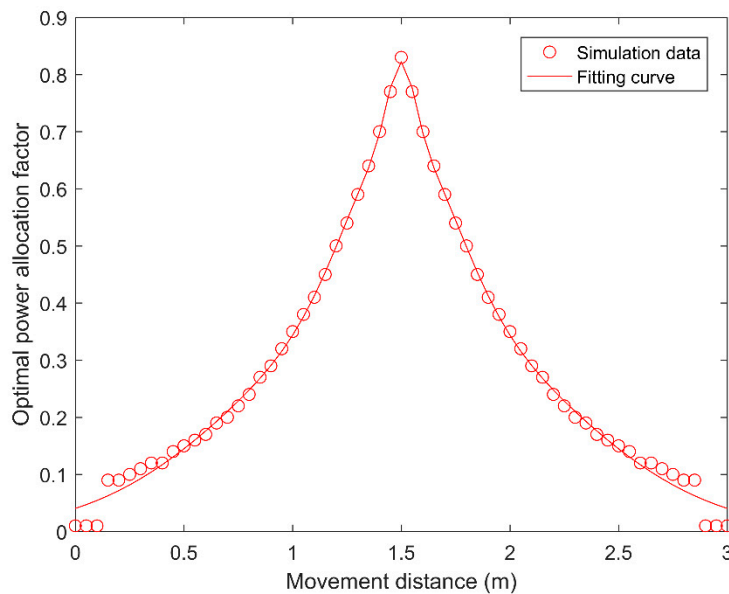

Figure 9. Optimal power allocation factor versus movement distance.

Moreover, according to the curve fitting, the fitting model can be expressed as

$$\alpha_{\text{optimal}} = \sum_{j=1}^{3} l_j \exp(-((\zeta - m_j)/n_j)2), \tag{26}$$

where α_{optimal} denotes the optimal power allocation factor; ζ denotes the movement distance of users; and the related coefficients l_j, m_j, and n_j are presented in Table 2.

Table 2. Coefficients used in Equation (26).

Coefficient	Value	Coefficient	Value	Coefficient	Value
l_1	0.1299	m_1	1.5	n_1	0.08495
l_2	0.2906	m_2	1.5	n_2	0.3375
l_3	0.4018	m_3	1.5	n_3	0.99

Next, we extend the model of the optimal power allocation factor to adapt to more realistic scenarios in which the transmitting power P_{elec} of the LED can be tunable. First, through simulations, we observe that under different values of P_{elec}, the variation of α_{optimal} along with movement distance may always be approximated as the sum of Gaussian functions as before, but with some shifting along the y-axis. Hence, we assume the extended model as follows:

$$\alpha_{\text{optimal}} = f(P_{\text{elec}}) + \sum_{j=1}^{3} l_j \exp(-((\zeta - m_j)/n_j)2). \tag{27}$$

In order to determine which functional form $f(P_{\text{elec}})$ obeys and the corresponding coefficients, we took the polynomial, exponential, and Gaussian function forms into account and created a function nlinfit() in MATLAB R2016a to perform nonlinear regression based on a data set. The resulting best-fitting model with an RMSE of 0.029 was

$$\alpha_{\text{optimal}} = t_1 + t_2 P_{\text{elec}} + t_3 P_{\text{elec}}^2 + t_4 P_{\text{elec}}^3 + \sum_{j=1}^{3} l_j \exp(-((\zeta - m_j)/n_j)2), \tag{28}$$

where the related coefficients t_1, t_2, t_3, t_4, l_j, m_j, and n_j are presented in Table 3.

Table 3. Coefficients in Equation (28).

Coefficient	Value
t_1	-0.0223
t_2	7.7957
t_3	-2.3387×10^3
t_4	1.8817×10^5
l_1	0.1249
l_2	0.2581
l_3	0.3609
m_1	1.5
m_2	1.5
m_3	1.5
n_1	0.0999
n_2	0.4032
n_3	1.1839

In order to verify the model's effectiveness under different P_{elec} values, we conducted a simulation, with the result shown in Figure 10.
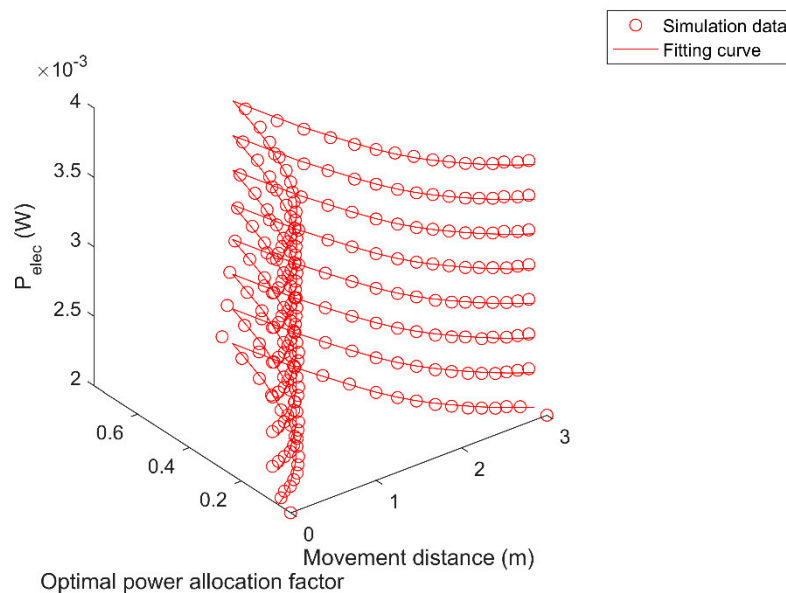

Figure 10. Optimal power allocation factor versus movement distance under different P_{elec} values.

7. Conclusions

In this paper, we put forward a novel concept named the "inverse power allocation (IPA)" which can lead to a higher total achievable data rate compared to conventional power allocation systems, at a cost of user fairness. Then, we proposed an adaptive power allocation scheme based on a MADM

algorithm, in which the total achievable data rate and user fairness were considered comprehensively via mathematical assessment; through simulation, the conditions under which the IPA scheme or the conventional scheme will be adopted were observed and the optimal power allocation factor was obtained according to users' locations. Finally, after assuming users walk along certain trajectories, we studied a variation model of the optimal power allocation factor along with users' movement distances utilizing the curve fitting technique and derived a fitting model.

Author Contributions: Conceptualization, Z.D. and T.S.; formal analysis, Z.D. and T.S.; funding acquisition, T.S.; investigation, Q.L. and T.T.; methodology, Z.D. and T.T.; software, Z.D. and T.T.; validation, T.S. and Q.L.; writing—original draft, Z.D. and Q.L.; writing—review and editing, Z.D. and T.S.

Conflicts of Interest: The authors declare no conflict of interest. The funders had no role in the design of the study; in the collection, analyses, or interpretation of data; in the writing of the manuscript, or in the decision to publish the results.

References

1. Andrews, J.G.; Buzzi, S.; Wan, C.; Hanly, S.V.; Lozano, A.; Soong, A.C.K. What will 5g be? *IEEE J. Sel. Areas Commun.* **2014**, *32*, 1065–1082. [CrossRef]
2. Jovicic, A.; Li, J.; Richardson, T. Visible light communication: Opportunities, challenges and the path to market. *IEEE Commun. Mag.* **2013**, *51*, 26–32. [CrossRef]
3. Burchardt, H.; Serafimovski, N.; Tsonev, D.; Videv, S.; Haas, H. VLC: Beyond point-to-point communication. *IEEE Commun. Mag.* **2014**, *52*, 98–105. [CrossRef]
4. Haas, H.; Yin, L.; Wang, Y.; Chen, C. What is LiFi? *IEEE J. Lightw. Technol.* **2016**, *34*, 1533–1544. [CrossRef]
5. Pathak, P.H.; Feng, X.; Hu, P.; Mohapatra, P. Visible light communication, networking, and sensing: A survey, potential and challenges. *IEEE Commun. Surv. Tutur.* **2015**, *17*, 2047–2077. [CrossRef]
6. Saito, Y.; Kishiyama, Y.; Benjebbour, A.; Nakamura, T.; Li, A.; Higuchi, K. Non-orthogonal multiple access (NOMA) for cellular future radio access. In Proceedings of the 2013 IEEE 77th Vehicular Technology Conference (VTC Spring), Dresden, Germany, 2–5 June 2013; pp. 1–5. [CrossRef]
7. Saito, Y.; Benjebbour, A.; Kishiyama, Y.; Nakamura, T. System level performance evaluation of downlink non-orthogonal multiple access (NOMA). In Proceedings of the 2013 IEEE 24th Annual International Symposium on Personal, Indoor, and Mobile Radio Communications (PIMRC), London, UK, 8–9 September 2013; pp. 611–615. [CrossRef]
8. Ding, Z.; Yang, Z.; Fan, P.; Poor, H.V. On the performance of non-orthogonal multiple access in 5G systems with randomly deployed users. *IEEE Signal Process. Lett.* **2014**, *21*, 1501–1505. [CrossRef]
9. Marshoud, H.; Kapinas, V.M.; Karagiannidis, G.K.; Muhaidat, S. Non-orthogonal multiple access for visible light communications. *IEEE Photonics Technol. Lett.* **2016**, *28*, 51–54. [CrossRef]
10. Yin, L.; Popoola, W.O.; Wu, X.; Haas, H. Performance evaluation of non-orthogonal multiple access in visible light communication. *IEEE Trans. Commun.* **2016**, *64*, 5162–5175. [CrossRef]
11. Guan, X.; Yang, Q.; Hong, Y.; Chan, C.C.K. Non-orthogonal multiple access with phase pre-distortion in visible light communication. *Opt. Express* **2016**, *24*, 25816–25823. [CrossRef] [PubMed]
12. Fu, Y.; Hong, Y.; Chen, L.K.; Sung, C.W. Enhanced power allocation for sum rate maximization in OFDM-NOMA VLC systems. *IEEE Photonics Technol. Lett.* **2018**, *30*, 1218–1221. [CrossRef]
13. Chen, C.; Zhong, W.D.; Yang, H.; Du, P. On the performance of MIMO-NOMA based visible light communication systems. *IEEE Photonics Technol. Lett.* **2018**, *30*, 307–310. [CrossRef]
14. Yin, L.; Wu, X.; Haas, H. On the performance of non-orthogonal multiple access in visible light communication. In Proceedings of the 2015 26th Annual Symposium on Personal, Indoor, and Mobile Radio Communications (PIMRC), Hong Kong, China, 30 August–2 September 2015; pp. 1354–1359. [CrossRef]
15. Zhang, X.; Gao, Q.; Gong, C.; Xu, Z. User grouping and power allocation for NOMA visible light communication multi-cell networks. *IEEE Commun. Lett.* **2017**, *21*, 777–780. [CrossRef]
16. Zeng, L.; O'Brien, D.C.; Minh, H.L.; Faulkner, G.E.; Lee, K.; Jung, D. High data rate multiple input multiple output (MIMO) optical wireless communications using white led lighting. *IEEE J. Sel. Areas Commun.* **2009**, *27*, 1654–1662. [CrossRef]

17. Kahn, J.M.; Barry, J.R. Wireless infrared communications. *Proc. IEEE* **1997**, *85*, 265–298. [CrossRef]

18. Andrews, J.G.; Meng, T.H. Optimum power control for successive interference cancellation with imperfect channel estimation. *IEEE Trans. Wirel. Commun.* **2003**, *2*, 375–383. [CrossRef]

19. Datasheet of BPW21R. Available online: https://pdf1.alldatasheetcn.com/datasheet-pdf/view/26249/VISHAY/BPW21R.html (accessed on 20 March 2019).

20. Wang, Y.M. A method based on standard and mean deviations for determining the weight coefficients of multiple attributes and its applications. *Appl. Stat. Manag.* **2003**, *22*, 22–26. [CrossRef]

21. Sheng-Mei, L.; Su, P.; Ming-Hai, X. An improved TOPSIS vertical handoff algorithm for heterogeneous wireless networks. In Proceedings of the 2010 IEEE 12th International Conference on Communication Technology (ICCT 2010), Nanjing, China, 11–14 November 2010; pp. 750–754. [CrossRef]

22. Lahby, M.; Cherkaoui, L.; Adib, A. Performance analysis of normalization techniques for network selection access in heterogeneous wireless networks. In Proceedings of the 2014 IEEE 9th International Conference on Intelligent Systems: Theories and Applications (SITA-14), Rabat, Morocco, 7–8 May 2014; pp. 1–5. [CrossRef]

23. James, G.; Witten, D.; Hastie, T.; Tibshirani, R. *An Introduction to Statistical Learning*; Springer: New York, NY, USA, 2013.